Simulations of a Hydrological Model as Coupled to a Regional Climate Model

ZENG Xinmin *[1,2](曾新民), ZHAO Ming [2](赵 鸣), SU Bingkai [2](苏炳凯), TANG Jianping [2](汤剑平), ZHENG Yiqun [1](郑益群), GUI Qijun [1](桂祁军), and ZHOU Zugang [1] (周祖刚)

[1] *Institute of Meteorology, P.L.A. University of Science and Technology, Nanjing* 211102

[2] *Key Laboratory for Mesoscale Severe Weather, the China Ministry of Education, Nanjing University, Nanjing* 210093

(Received January 8, 2002; revised November 15, 2002)

ABSTRACT

Considering a detailed hydrologic model in the land surface scheme helps to improve the simulation of regional hydro-climatology. A hydrologic model, which includes spatial heterogeneities in precipitation and infiltration, is constructed and incorporated into the land surface scheme BATS. Via the coupled-model (i.e., a regional climate model) simulations, the following major conclusions are obtained: the simulation of surface hydrology is sensitive to the inclusion of heterogeneities in precipitation and infiltration; the runoff ratio is increased after considering the infiltration heterogeneity, a result which is more consistent with the observations of surface moisture balance over humid areas; the introduction of the parameterization of infiltration heterogeneity can have a greater influence on the regional hydro-climatology than the precipitation heterogeneity; and the consideration of the impermeable fraction for the region reveals some features that are closer to the trend of aridification over northern China.

Key words: hydrological model, spatial heterogeneity, moisture balance, regional climate, sensitivity test

1. Introduction

Recently, studies on the global change of the interactions between the hydrosphere, biosphere, and atmosphere have attracted extensive attention, and more and more international investigations are recognizing the importance of including the heterogeneities in the hydrological processes (e.g., the features of soil texture, precipitation, and topography) into the land surface schemes (Famiglietti and Wood, 1994; Peters-Lidard et al., 1997; Walko et al., 2000). Until now, the inter-disciplinary simulation studies of hydro-climatology that consider the spatial variability of hydrology, have seldom been reported in China, while detailed hydrological models are generally limited to one-way coupling studies. Many basin hydrological models have been developed in China (Zhao, 1984; Li, 1998), which are applied to hydrological forecasting, yet they only use the meteorological characteristics of observations or outputs of atmospheric models as the input forcings into themselves, while the calculated quantities from the hydrological models (e.g., evaporation and soil moisture) do not feed back into the atmospheric models. All these hydrological models are off-line tests (one-way coupling), and cannot be directly used in climate models. In fact, only the two-way coupling models can simulate the complex nonlinear interactions. Better simulations for surface hydrology can improve the precision of modeling of the climate, and vice versa. In some investigations, e.g., forecasting the future climate and estimating the future water resources, the coupling study is of particular importance.

This paper intends to consider two pronounced spatial heterogeneities among many heterogeneities, i.e., the heterogeneities in precipitation and infiltration over a grid area (60 km × 60 km) in the hydrological component of the climate model.

With regard to precipitation heterogeneity, observations show that precipitation differs in precipitation amount and precipitating area due to different natures. The simulated amounts of precipitation and runoff are often underestimated in climate models that neglect precipitation heterogeneity (Entekhabi and Ea-

*E-mail: zen_xm@yahoo.com

gleson, 1989). Eagleson et al. (1987) studied the wetted fraction (μ) within a grid area due to precipitation, and demonstrated that about 60% of the storm area is covered by precipitation, while for a general-circulation-model (GCM) grid, about half of the grid area is wetted by typical storms. Besides, among studies of precipitation amount within a grid area, Warrilow et al. (1986) assumed an exponential distribution to represent the precipitation heterogeneity, which was followed by many others (e.g., Entekhabi and Eagleson, 1989; Zhang and Ding, 1998), while Gao and Sorooshian (1994) found that the log-normal distribution is more consistent with the observations in some cases.

With regard to infiltration capacity, some formulae (e.g., Horton's and Phillip's formulae) are representative. However, these formulae often ignore the infiltration heterogeneity and are generally applied to very uniform soil. The Xinanjiang Model (Zhao, 1984) considers the heterogeneity in infiltration capacity mainly due to soil texture, and the parameterization scheme is also applied in other investigations (Francini and Pacciani, 1991; Wood et al., 1992; Stamm and Wood, 1994; Liang et al., 1996), among which the Variable Infiltration Capacity (VIC) model originally developed in the Geophysical Fluid Dynamics Laboratory (GFDL) was applied to the coupling with low-spatial resolution GCMs without considering the influences of the biosphere.

In this paper, a hydrological model is developed based on consideration of the heterogeneities in the hydrological processes. The model is then coupled to the regional climate model RegCM2 (Giorgi et al., 1993a, b) so as to improve the ability to simulate the regional hydro-climatology at relatively small spatial scales and to analyze the sensitivities of the model to the hydrological-process heterogeneities.

2. Brief description of the model

2.1 *An off-line hydrological model*

A hydrological model VXM (a combination of the VIC and Xinanjiang Models) is developed, which combines the parameterization of the VIC model to that of the Xinanjiang Model. It is an off-line, one soil-layer model considering two water sources (surface runoff and ground runoff) with two case treatments (homogeneous and heterogeneous) for precipitation.

2.1.1 *Homogeneous precipitation case*

VXM considers the heterogeneity in infiltration capacity (defined as the maximum depth of the water that the soil column can retain), and therefore the heterogeneities in runoff and evapotranspiration are induced. The infiltration heterogeneity can be induced by many factors such as the heterogeneities in soil properties, topography, and vegetation over a given area (e.g., a grid area). Therefore over a given area, the heterogeneity in the infiltration capacity i can be represented by Stamm and Wood (1994):

$$i = i_{\mathrm{m}}\left[1-(1-A)^{1/B}\right], \tag{1}$$

where A is the ratio of the area with the infiltration capacity lower than i to the entire area ($0 \le A \le 1$), i_{m} is the maximum infiltration capacity within the entire area, and B denotes the shape parameter of the infiltration curve (Fig. 1). Thus, given an initial value (or a value prior to a time step) i=i_0, Q_{d}, the surface runoff corresponding to P, a precipitation amount within a time step over the area, can be written as

$$Q_{\mathrm{d}} = \int_{i_0}^{i_0+P} A\,(i)\,di. \tag{2}$$

In fact, Q_{d} is the proportion of the precipitation amount P that precipitates to the saturated area A_{s}, and therefore the infiltration amount is $P-Q_{\mathrm{d}}$. Then, the maximum soil water storage W_{c} and the initial soil water storage W_0 can be derived from

$$W_c = \frac{i_{\mathrm{m}}}{1+B}, \tag{3}$$

and

$$W_0 = W_c\left[1-\left(\frac{i_{\mathrm{m}}-i_0}{i_{\mathrm{m}}}\right)^{B+1}\right]. \tag{4}$$

Thus, if the values of the parameters B and W_{c} are given, and initially i=i_0, and the precipitation amount is P within a time step, then the surface runoff within a time step, Q_{d}, is

$$Q_d = \begin{cases} P - W_c + W_0, & \text{if } i_0 + P \ge i_{\mathrm{m}} \\ P - W_c + W_0 + W_c\left[1-\dfrac{i_0+P}{i_{\mathrm{m}}}\right]^{1+B}, & \text{if } i_0 + P < i_{\mathrm{m}}. \end{cases} \tag{5}$$

Following Stamm and Wood (1994), the evapotranspiration in VXM is

$$E = E_{\mathrm{p}}\left[1-\left(1-\frac{W_0}{W_c}\right)^{1/B_{\mathrm{e}}}\right], \tag{6}$$

where E_{p} is the maximum evapotranspiration within a time step, and B_{e} is a characteristic parameter for evapotranspiration. As for the base flow in the one-layer model, the linear reservoir is applied (Stamm and Wood, 1994):

$$Q_b = k_b W_0, \tag{7}$$

where $0 \leq k_b \leq 1$.

The above equations should be modified for the impermeable fraction inthe basin. If only precipitation and evapotranspiration are considered over the fraction f_i, which denotes the ratio of the impermeable area to the entire area of the basin, then the precipitation is $P \times (1 - f_i)$. With a time step of 200 s, the evapotranspiration e_i (in mm) is calculated by

$$e_i = \min\left[\max\left(4 \times 10^{-4} f_i, 0.08 f_i P\right), f_i E_p\right]. \tag{8}$$

Therefore, the total evapotranspiration is

$$E = e_i + E_p\left[1 - \left(1 - \frac{W_0}{W_c}\right)^{1/B_e}\right](1 - f_i). \tag{9}$$

In addition, W_c is not modified here because the same infiltration/runoff-generation curve (Fig. 1) is also assumed to be satisfied over $(1 - f_i)$, the permeable fraction, which is different from Zhao (1984). That is to say, the same equation for the infiltration heterogeneity is considered, and other quantities can be obtained via the same method as the case of treating the whole basin as a permeable area, except that some quantities such as i_0 and W_c are considered over the permeable fraction only.

Thus, B, W_c, B_e, k_b, and f_i are the major parameters of the model. Given the values of these parameters and some parameters that are related to the time step (e.g., i_0, E_p, and P), the quantities of interest, such as the surface runoff Q_d and soil water storage W_0, can be computed.

2.1.2 *Heterogeneous precipitation case*

As for the treatment of heterogeneous precipitation, the large-scale precipitation is assumed to be uniformly distributed, while only cumulus convective precipitation is treated as a heterogeneous distribution. The reason for this is that precipitation heterogeneity is mainly caused by cumulus convection.

The cumulus convective heterogeneous precipitation case in VXM is analogous to the homogeneous precipitation case, where the only difference is that now the equations include precipitation heterogeneity. Similar to Warrilow et al. (1986), the precipitation heterogeneity is assumed via an exponential distribution over the precipitating area (represented by a normalized fraction) for the precipitation intensity. A relatively small time step, i.e., about 3 minutes, is taken here, hence it is natural to assume the precipitation intensity is exponentially distributed within the time interval according to

$$f(P_k) = \frac{\mu}{P_c}\exp\left(-\frac{\mu P_k}{P_c}\right), \tag{10}$$

where $f(P_k)$ is the probability density function of P_k, μ is the ratio of the area receiving the cumulus convective precipitation amount P_c to the entire area of the grid. Setting x in the range of μ to be the ratio of the area with a precipitation amount larger than P_k to the entire precipitating area within a time step, then

$$\begin{aligned} x &= 1 - \int_0^{P_k} f(P_k) dP_k \\ &= \exp\left(-\frac{\mu P_k}{P_c}\right). \qquad 0 < x \leq 1. \end{aligned} \tag{11}$$

Similar to the case of homogeneous precipitation, the differential coefficient of surface runoff within the time step is

$$dQ_d = \begin{cases} [P_k(x) - W_c + W_0]dx, & i_0 + P_c \geq i_m \\ \left[P_k(x) - W_c + W_0 + W_c\left(1 - \dfrac{i_0 + P_c}{i_m}\right)^{1+B}\right]dx, & i_0 + P_c < i_m. \end{cases} \tag{12}$$

If the areal fraction a satisfies $i_0 + P_k(a) = i_m$, respectively integrating the above equation over the two intervals and summing them yields the surface runoff induced by convective precipitation within a time step

$$Q_d = P_c - \mu(W_c - W_0) + \mu W_c \int_a^1 \left[1 - i_0 - \frac{P_c}{\mu}\ln x / i_m\right]^{1+B} dx. \tag{13}$$

as is similar to Liang et al. (1996).

The value of the above integral equation is not difficult to solve via a numerical method (Liang et al., 1996). Computing other quantities for the heterogeneous precipitation case (e.g., W_0 and E) are analogous to the homogeneous precipitation case.

It should be noted that in this case, the total surface runoff within a time step is made up of two surface runoffs, namely the one induced by cumulus convection from (13), and the other caused by large-scale precipitation from (5).

For each characteristic parameter of VXM, some tests are designed (not shown) which show that the model is quite (or very) sensitive to the parameters, i.e., k_b, μ, f_i, W_0, and W_c.

2.2 *Coupling the hydrological model to a regional climate model*

One of the most representative regional climate models is RegCM2 (Giorgi et al., 1993a, b) developed by the National Center for Atmospheric Research (NCAR), which employs the land surface scheme BATS (the Biosphere/Atmosphere Transfer Scheme, Dickinson et al., 1993). There is no description for the hydrological heterogeneity in BATS. Furthermore, the surface runoff rate in BATS, R_s, is assumed to be a simple function of the relative saturation of soil water in the surface layer and rooting zone, and it is after the computation of R_s that the infiltration rate is calculated. In terms of the physical process, it is the water (from precipitation or melting snow) that cannot infiltrate into the soil that forms surface runoff. Apparently, the surface treatment is very empirical and not physically based. To make the hydrological processes more physically based and to improve the description of the hydrological processes at the regional scale, enhancing the ability simulating or forecasting the regional hydro-climatology, VXM is slightly modified and then incorporated into RegCM2. Because the treatment of runoff is the key to the hydrological models (Zhao, 1984), VXM is not used to replace the original version of BATS, which is employed in RegCM2, but modified when it is incorporated (i.e., computationally, the only effect of VXM is its substitution for surface runoff in BATS when it is incorporated, while the computations of momentum and sensible and latent heat fluxes remain the same as in the original BATS scheme). Therefore, the incorporated modified VXM as well as the original components of soil moisture movement and vegetative transpiration in BATS form an integrated two-way coupled hydrological model, and the soil-vegetation-atmosphere interactions are thus included in the model.

According to the choices of the VXM parameter values and the setting of the BATS parameters, the water storage W_c varies between 120 and 160 mm, with higher values in northern China and lower values in southern China for the grid areas. Additionally, the initial value W_0 corresponds to the initialization scheme in BATS.

3. Modeling experiment

3.1 *Experimental design*

The model domain is centered at (117.00°E, 35.20°N), with a horizontal resolution of 60 km ×60 km, a horizontal grid mesh of 41×40, and an area range within 24.7° – 45.7°N and 100.88° – 33.12° E

Table 1. Parameter values prescribed in the experiments

	EXP1 and EXP13	EXP2 and EXP14	EXP3 and EXP15	EXP4 and EXP16	EXP5 and EXP17	EXP6 and EXP18	EXP7 and EXP19	EXP8 and EXP20	EXP9 and EXP21	EXP10 and EXP22	EXP11 and EXP23	EXP12 and EXP24
μ		—	0.4	0.6	0.8	1.0	—	0.6	1.0	—	—	0.6
B	—	0.3	0.3	0.3	0.3	0.3	0.3	0.3	0.3	0.15	0.5	0.3
f_i	—	0.	0.	0.	0.	0.	0.	0.	0.	0.	0.	0.15
k_b	—	5×10^{-5}	5×10^{-5}	5×10^{-5}	5×10^{-5}	5×10^{-5}	10^{-4}	10^{-4}	10^{-4}	10^{-4}	10^{-4}	5×10^{-5}

Table 1 lists some values of the parameters of the coupled model, where μ denotes the fraction of the area of the cumulus convective precipitation relative to the grid area, and the large-scale precipitation is assumed homogeneous. According to the values and the scheme described above, the first group of experiments (EXP1-EXP12) are simulations using the 1991 warm season (May, June, and July) station observations as the initial and boundary conditions. Correspondingly, the second group of experiments (EXP13-EXP24) apply the 1998 warm season (May, June, and July) NCEP/NCAR reanalysis data as the initial and boundary conditions. Among the experiments, EXP1 and EXP13 employ the original version RegCM2, while the regional climate model, which includes the above hydrological model considering the heterogeneities and is two-way coupled, is applied for the other experiments. Note that in each experiment of the same group, the initial and boundary conditions as well as the options of the model physics are the same.

3.2 *Preliminary analysis of the simulations*

The experiments with $k_b = 5 \times 10^{-5}$ (i.e., EXP1-EXP6 and EXP13-EXP18) are mainly discussed, in which EXP1 and EXP13 do not consider heterogene-

ity and are performed with the original model, EXP2 and EXP14 do not consider the precipitation heterogeneity, and the other four in each group consider the precipitation and infiltration heterogeneities with the precipitation coverage increasing gradually. In addition, EXP4 and EXP16 are taken as the control experiments for each group respectively.

Figure 2 compares the simulated precipitation field with the observed one. It is shown that after the inclusion of the precipitation and infiltration heterogeneities, the coupled model can successfully reproduce the typical Meiyu rainbelt occurring in the Changjiang-Huaihe Valley (denoted as the JHR region). It should be noted that there is a so-called "numerical point storm" (Giorgi, 1991; Liu and Avissar, 1996) over the sea surface around (127°E, 32°N), whose formation may be related to the parameterization scheme for precipitation. Besides, due to the same lateral-boundary forcings, the simulated stream flow and temperature fields are also consistent with the observed ones (not shown).

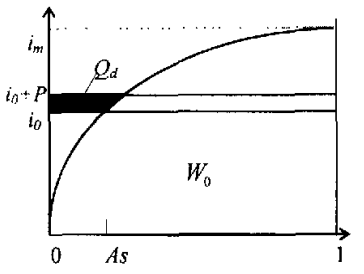

Fig. 1. Schematic of runoff-infiltration relationships for VXM (the permeable-area case).

Table 2. Simulated characteristic quantities for the JHR region (around the Changjiang-Huaihe River Valley), in which P_m, R_m, P_a, and r_a represent the maximum 3-month accumulated precipitation, maximum 3-month accumulated surface runoff, areally-averaged 3-month-mean precipitation and the ratio of the areally-averaged 3-month-mean surface runoff to the corresponding precipitation, respectively

	EXP1 (EXP13)	EXP2 (EXP14)	EXP3 (EXP15)	EXP4 (EXP16)	EXP5 (EXP17)	EXP6 (EXP18)	EXP7 (EXP19)	EXP8 (EXP20)	EXP9 (EXP21)	EXP10 (EXP22)	EXP11 (EXP23)	EXP12 (EXP24)
P_m(mm)	1439 (1376)	1523 (1361)	1625 (1374)	1566 (1414)	1352 (1396)	1683 (1415)	1544 (1366)	1383 (1339)	1375 (1402)	1575 (1419)	1637 (1371)	1594 (1398)
R_m(mm)	691 (528)	1188 (1057)	1158 (933)	1243 (1083)	1067 (1095)	1419 (1116)	1210 (1004)	1017 (967)	1044 (1051)	1232 (1063)	1298 (1014)	1327 (1106)
P_a(mm)	538 (663)	540 (655)	550 (665)	524 (663)	532 (665)	545 (657)	534 (661)	545 (668)	538 (662)	548 (664)	532 (657)	524 (671)
r_a(%)	28.0 (31.1)	50.2 (55.6)	40.6 (48.1)	49.2 (54.5)	51.8 (58.1)	51.6 (56.9)	45.0 (50.7)	45.4 (50.9)	46.6 (52.0)	44.4 (49.7)	46.8 (51.8)	55.4 (61.2)

Shown in the 3-month-accumulated precipitation, the differences in the spatial distribution of precipitation may be quite large (e.g., P_m in Table 2) for the same group of experiments, but the regional averages display little difference (e.g., P_a in Table 2). This is because the model solution for the interior of the domain is basically determined by the dynamical equilibrium of the lateral boundaries and the model physics (Giorgi and Mearns, 1999), and among the factors in the equilibrium, land surface heterogeneity is less important in affecting the atmospheric variables. Due to the heterogeneity effects, the variance of precipitation may be quite large at relatively small time-space scales (e.g., at the pentad scale over a small region), while at a larger time-space scale (e.g., over the model domain at the seasonal scale), the variation of precipitation may be quite small due to the same lateral-boundary forcings and model physics.

The difference between EXP1 and EXP2 (EXP13 and EXP14) only lies in that EXP2 (EXP14) considers the infiltration heterogeneity, and the differences among EXP2-EXP6 (EXP14-EXP18) lies in whether the precipitation heterogeneity is considered or the extent of the heterogeneity. From r_a in Table 2, the difference between EXP1 and EXP2 is the largest compared with the difference between EXP2 and one of EXP3-EXP6. Therefore, the effects of the incorporation of the infiltration heterogeneity into RegCM2 are larger than those of the precipitation heterogeneity. This is because the differences in regional-average precipitation among the different experiments are small, yet the change in the nature of infiltration can pro-

nouncedly alter the land surface hydro-climatology. Similarly, from the comparisons of other quantities such as surface fluxes (Table 3) and surface temperature (Fig. 3), the largest differences are between the experiment with the inclusion of the infiltration heterogeneity and that without the inclusion.

From the differences between the results of EXP13 and those of EXP14, the effects of the infiltration heterogeneity only can be seen. The 3-month-mean 850 hPa temperatures in EXP13 are 0.3°C lower than those in EXP14 over the greater part of the JHR region, and the surface temperatures in EXP13 are 0.4–1.7°C lower than those in EXP14 (Fig. 3). All of this shows that the infiltration greatly influences the air and soil temperatures, and that the land surface and low-level-air temperatures are increased after the mere infiltration heterogeneity is taken into account in the model. This effect is due to the increase of runoff (i. e., the increase of r_a) and the decrease of infiltration, therefore the soil moisture and the soil heat storage are decreased, which causes the soil surface temperature to rise and further leads to higher surface temperature in EXP14 compared with EXP13. Similar results can be seen from the simulations of EXP1 and EXP2 (not shown).

It can be seen that the simulated results are also

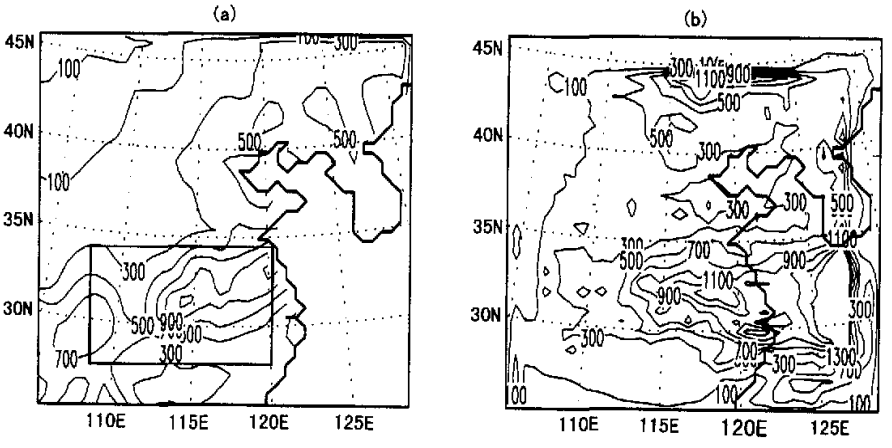

Fig. 2. 3-month accumulated precipitation of EXP4 and the corresponding observations (a) observed; (b) simulated. (units: mm; area within the rectangle of panel (a) denotes the JHR region).

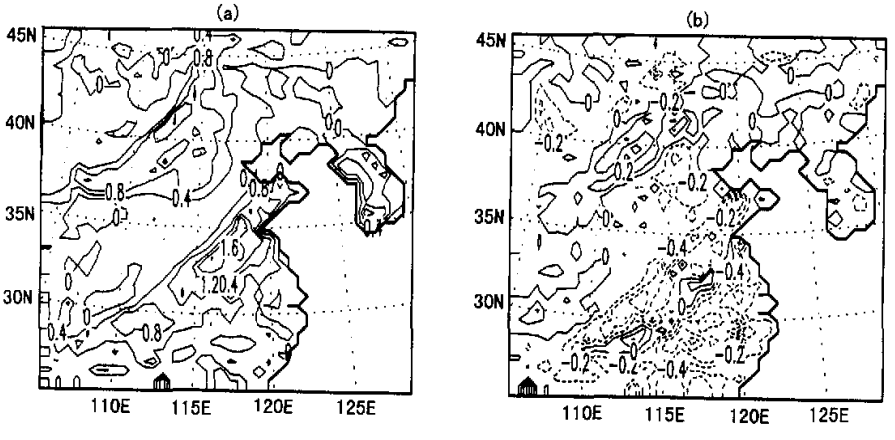

Fig. 3. 3-month-mean surface temperature differences simulated after the infiltration heterogeneity is included (a) difference between EXP14 and EXP13 with a contour interval of 0.4°C; (b) difference between EXP14 and EXP16 with an interval of 0.2°C.

Table 3. Simulated differences in areally-averaged 3-month-mean fluxes for the JHR region. (SHF: sensible heat flux; LHF: latent heat flux; units: W m^{-2})

Land surface fluxes	EXP2–EXP1 (EXP14–EXP13)	EXP2–EXP3 (EXP14–EXP15)	EXP2–EXP4 (EXP14–EXP16)	EXP2–EXP5 (EXP14–EXP17)	EXP2–EXP6 (EXP14–EXP18)
SHF(W m^{-2})	8.5	3.8	−2.5	4.4	−2.0
	(6.1)	(3.9)	(−1.2)	(1.3)	(−0.4)
LHF(W m^{-2})]	−13.1	−0.6	3.2	−3.7	2.4
	(−7.2)	(−3.2)	(1.3)	(−2.3)	(0.6)

sensitive to the precipitation heterogeneity. Shown from the maximum pentad surface runoff in Table 4, the differences between EXP5 and EXP2 are very large in the 4th and 5th pentads. Thus, due to the different extent of precipitation heterogeneity, the hydrological processes at the pentad scale may display large differences, and the distributions of the regional precipitation may differ greatly as well. In addition, the differences in the extent of precipitation heterogeneity can also affect other characteristic quantities via the interactions between the hydrological and the atmospheric processes (not shown).

Listed in Table 2, the values of r_a, the ratio of the regional average of the 3-month-accumulated surface runoff to that of the corresponding precipitation, are 28.0% in EXP1 and 31.1% EXP13, and are larger than 40% in other experiments (e.g., 49.2% and 54.5% in the control experiments EXP4 and EXP16, respectively). The result that the inclusion of infiltration heterogeneity leads to the increase in the runoff is in good agreement with the observed climate, e.g., the ratios of runoff to precipitation in May, June, and July are larger than 40% in the Wuhan station of Central China (Fig.4), which is consistent with the simulated result with the infiltration heterogeneity included. Moreover, considering that extremely severe floods occurred in the Yangtze River Valley in the years 1991 and 1998, the runoff ratios are also in agreement with the facts. Liu et al. (1994) simulated the regional climate of June, July, and August in China with the original version RegCM2, showing that the 3-month surface runoff is very close to 20% in Central China where the JHR region is located. Since the year 1991 is normal in terms of climate, while the climates in 1991 and 1998 have wet biases compared with the multi-year climate, the result in Liu et al.(1994) is quite consistent with the results of EXP1 and EXP13. Therefore, the original version RegCM2 underestimates the runoff in southern China, while the simulations of the modified version are relatively close to observations.

Table 4. Simulated maximum pentad surface runoff ratio for the JHR region (units: mm)

Pentad	EXP1	EXP2	EXP3	EXP4	EXP5	EXP6
1	11.5	12.0	13.1	15.5	13.2	14.3
2	24.7	24.2	21.3	24.4	23.7	27.0
3	8.4	8.5	9.3	9.7	10.2	10.6
4	57.4	105.7	87.9	36.6	41.9	67.1
5	141.0	243.4	222.0	212.5	417.3	230.6
6	72.9	112.5	95.3	114.3	100.1	82.1
7	80.3	134.3	99.1	121.2	93.2	175.2
8	129.4	166.6	161.7	185.9	180.8	187.4
9	236.4	432.7	305.2	389.8	403.1	421.8
10	79.4	135.0	101.9	173.8	172.9	205.1
11	27.5	77.9	50.2	42.7	78.3	56.5
12	59.4	221.0	163.0	235.5	217.2	238.7
13	315.7	453.3	490.7	552.8	495.8	518.1
14	250.8	352.5	428.1	400.1	396.3	406.6
15	306.2	311.3	281.4	240.7	318.6	349.0
16	227.7	384.3	333.2	367.1	390.7	411.4
17	72.3	113.7	78.5	69.5	90.1	103.8
18	147.8	304.3	286.5	240.8	241.8	366.3

The other experiments also demonstrate that the model is sensitive to the parameters (not shown), e.g., B and W_c. Here the experimental results for f_i, the impermeable fraction only, are given. Since the climate over the semi-arid regions is often dry with hardened soils, the parameter f_i is necessary to describe the regions (Zhao, 1984). The conditions for the sensitivity experiments EXP4 and EXP12 are the same except that the values of f_i are taken to be 0. and 0.15, respectively. Shown in Table 2, the runoff ratios in EXP12 and EXP24 are the largest in the experiments given, due to $f_i > 0$ in the two experiments. Thus, the increase of the impermeable fraction leads to the increase of runoff (Fig. 5a), then to the decrease of soil moisture, and therefore to the rise of the surface temperature (Fig. 5b). Displayed by the magnitude of the rise of the surface temperature (Fig. 5b), the

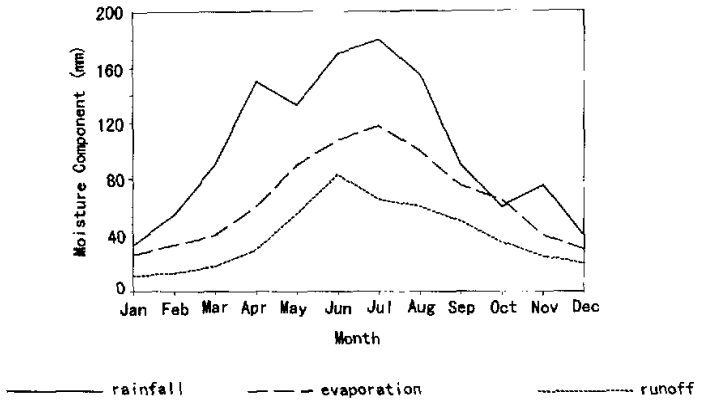

Fig. 4. Observed annual-mean surface moisture balance components in Wuhan (units: mm).

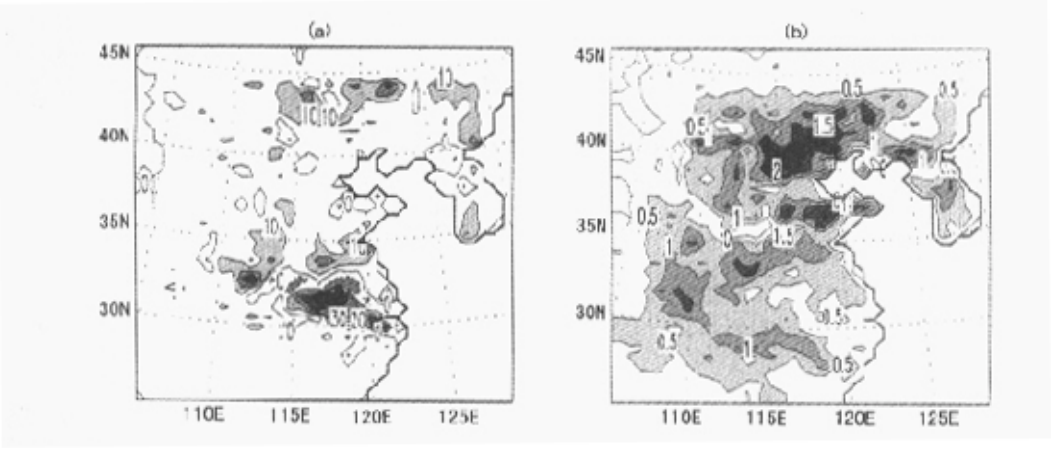

Fig. 5. The difference in simulated results between EXP4 and EXP12, (a) the difference in 3-month-accumulated surface runoff (contour interval: 10 cm), (b) the difference in 3-month-mean surface temperature (contour interval: 0.5°C).

model is quite sensitive to the parameter f_1. The feature that the soil moisture is decreased along with the rise of temperature is consistent with the trend of aridification, which further confirms the need to include the parameter f_1 for the semi-arid regions via coupled-model simulations.

4. Conclusions

In this paper, a hydrological model that considers the precipitation and infiltration heterogeneities is developed and then incorporated into the regional climate model RegCM2. The observational data for the 1991 warm season and the NCEP/NCAR reanalysis data for the 1998 warm season are used as the initial and boundary conditions in the 24 coupled-model simulations.

Results show that the hydrological processes are sensitive to the precipitation and infiltration heterogeneities, i.e., quite large changes in the simulations for soil moisture, soil temperature, and runoff may be induced due to the inclusion of the two heterogeneities. Due to the fact that the change in precipitation over monthly and seasonal scales is small, the distribution of infiltration is changed, which affects the distributions of runoff and the soil moisture and further in-

duces change in the surface temperature after different extents of the sub-grid precipitation and infiltration heterogeneities are accounted for.

The simulations for the hydrological processes are improved after the infiltration heterogeneity is considered, i.e., the runoff ratio is greatly enhanced compared to the original model. This is consistent with the reality of the moisture balance in the humid regions and is necessary for the model in evaluating the variations of the future regional climate and water resources. Due to the small changes in precipitation over monthly to seasonal scales, the increase of runoff leads to a decrease in soil moisture and heat storage, and further induces a rise in simulated surface temperature with the infiltration heterogeneity included. In addition, the impacts of the precipitation heterogeneity on the hydrological processes over the pentad scale are very large, and the effects of including the infiltration heterogeneity in the model on the regional hydroclimatology are greater than those of the precipitation heterogeneity in this study.

With the inclusion of the impermeable fraction in the model, the simulated results show an increase in the soil moisture and in the surface temperature, which is consistent with the aridification trend over northern China. This also confirms the need to consider the impermeable areas in the model for the semi-humid regions.

It should be noted that because only two sets of data were applied in the 24 coupled-model simulations and the analysis of each experiment covers the whole simulatation period, the results discussed include some information about the initial conditions, which does not fully show the effects of the model physics and may also decrease the sensitivity of the regional climate model to the incorporation of the hydrological model. The limitation induced by using the same initial conditions should be considered in the follow-up studies.

Acknowledgments. This work was jointly supported by the National Natural Science Foundation of China under Grant No. 40205012, and 40201048, the Chinese NKBRSF Project G1999043400 and the Foundation of the China Ministry of Education (Grant No. 20010284027). The computation of this work was implemented on the SGI computer of Nanjing University.

REFERENCES

Dickinson, R. E., A. Henderson-Sellers, P. J. Kennedy, and M. F. Wilson, 1993: Biosphere/Atmosphere Transfer Scheme (BATS) Version 1e as Coupled to the NCAR Community Climate Model. NCAR Tech. Note TN-387+STR, National Center for Atmospheric Research, Boulder, CO.

Eagleson, P. S., N. M. Fennessey, Q. Wang, and I. Rodriguez-Iturbe, 1987: Application of Poisson models to air mass thunderstorm rainfall. *J. Geophys. Res.*, **92**, 9661–9678.

Entekhabi, D., and P. Eagleson, 1989: Land surface hydrology parameterization for the atmospheric general models including subgrid-scale spatial variability. *J. Climate*, **2**, 816–831.

Famiglietti, J. S., and E. F. Wood, 1994: Multiscale modeling of spatially variable water and energy balance processes. *Water Resour. Res.*, **30**, 3061–3078.

Francini, M., and M. Pacciani, 1991: Comparative analysis of several conceptual rainfall-runoff models. *J. Hydrol.*, **122**, 161–219.

Gao, X., and S. Sorooshian, 1994: A stochastic precipitation dis-aggregation scheme for GCM applications. *J. Climate*, **7**, 238–247.

Giorgi, F., 1991: Sensitivity of simulated summertime precipitation over the western United States to different physics parameterizations. *Mon. Wea. Rev.*, **119**, 2870–2888.

Giorgi, F., M. R. Marinucci, and G. T. Bates, 1993a: Development of a second generation regional climate model (RegCM2): Boundary layer and radiative transfer processes. *Mon. Wea. Rev.*, **121**, 2794–2813.

Giorgi, F., M. R. Marinucci, G. DeCanio, and G. T. Bates, 1993b: Development of a second generation regional climate model (RegCM2), Cumulus cloud and assimilation of lateral boundary conditions. *Mon. Wea. Rev.*, **121**, 2814–2832.

Giorgi, F., and L. O. Mearns, 1999: Introduction to special section: Regional climate modeling revisited. *J. Geophys. Res.*, **104**, 6335–6352.

Li, Q., 1998: Analysis and discussion related to the hydrological watershed models used in the First Hydrological Forecasting Technology Competition of China. *Advances in Water Science*, **9**, 187–195 (in Chinese).

Liang, X., D. P. Lettenmaier, and E. F. Wood, 1996: One-dimensional statistical dynamic representation of subgrid spatial variability of precipitation in the two-layer variable infiltration capacity model. *J. Geophys. Res.*, **101**, 21403–21422.

Liu, Y., F. Giorgi, and W. M., Washington, 1994: Simulation of summer monsoon climate over East Asia with an NCAR regional climate model. *Mon. Wea. Rev.*, **122**, 2331–2348.

Liu, Y., and R. Avissar, 1996: Simulation with the regional climate model RegCM2 of extremely anomalous precipitation during the 1991 east Asian flood: An evaluation study. *J. Geophys. Res.*, **101**, 26199–26215.

Peters-Lidard, C. D., M. S. Zion, and E. F. Wood, 1997: A soil-vegetation-atmosphere transfer scheme for modeling spatially variable water and energy balance processes, *J. Geophys. Res.*, **102**, 4303–4324.

Stamm, J. F., and E. F. Wood, 1994: Sensitivity of a GCM simulation of global climate to the representation of land-surface hydrology. *J. Climate*, **7**, 1218–1239.

Walko, R. L., L. E. Band, and J. Baron, T. G. F. Kittel, R. Lammers, T. J. Lee, D. Ojima, R. A. Pielke Sr., C. Taylor, C. Tague, C. J. Tremback, and P. L. Vidale, 2000: Coupled atmosphere-biophysics-hydrology models for environmental modeling. *J. Appl. Meteor.*, **39**, 931–944.

Warrilow, D.A., A. B. Sangster, and A. Slingo, 1986: Modeling land surface processes and their influence on European climate. *Dyn. Clim. Tech. Note*, **38**, U. K. Meteor. Off., Bracknell, Berkshire, England, 92 pp.

Wood, E. F., D. P. Lettenmaier, and V. G. Zartarian, 1992: A land-surface hydrology parameterization with subgrid variability for general circulation models. *J. Geophys. Res.*, **97**, 2717–2728.

Zhang, J., and Y. Ding, 1998: An improved land-surface processes model and its simulation experiment: Part I: Land-processes model (LPM-ZD) and its "off-line" tests and performance analyses. *Acta Meteorologica Sinica*, **56**, 1–19. (in Chinese)

Zhao, R., 1984: *Basin Hydrologic Models—The Shanbei Model and the Xinanjiang Model*, The Electric-Power and Water-Conservancy Press, China, 180pp. (in Chinese)

一个水文模型与区域气候模式耦合的数值模拟研究

曾新民 赵 鸣 苏炳凯 汤剑平 郑益群 桂祁军 周祖刚

摘 要

在陆面过程方案中考虑精细的水文模型有助于改善对区域水文及气候的模拟。建立了一个考虑降水及入渗空间非均匀性的水文模型，并将其并入陆面过程方案BATS中。通过区域气候模式耦合模拟试验，得到如下主要结论：陆面水文的模拟对降水及入渗空间非均匀性的考虑非常敏感；考虑入渗非均匀性后，提高了径流系数，这与湿润地区水分平衡的观测结果更一致；入渗非均匀参数化方案的引入对区域水文及气候模拟的影响比降水非均匀参数化方案的引入要大；不透水面积在区域中的考虑所揭示的特征与我国北方干旱化趋势是一致的。

关键词：水文模型，空间非均匀性，水量平衡，区域气候，敏感性试验